



Study on Smoke Propagation Characteristics of a Carriage Fire in Longitudinally Ventilated Tunnel

Wei Cong, State Key Laboratory of Mining Response and Disaster Prevention and Control in Deep Coal Mines, Anhui University of Science and Technology, Huainan 232001 Anhui, China

Xudong Cheng, Long Shi and Kun He, State Key Laboratory of Fire Science, University of Science and Technology of China, Hefei 230026 Anhui, China*

Received: 31 July 2023/**Accepted:** 13 February 2024/**Published online:** 23 March 2024

Abstract. Model-scale experimental tests and numerical simulations were conducted to investigate the characteristics of the smoke overflow at the lateral carriage doors and the smoke temperature below the tunnel ceiling of a carriage fire in a longitudinally ventilated tunnel. Results indicate that the smoke overflows from the carriage into the tunnel through the lateral doors downstream of the fire source under the impact of longitudinal ventilation. Depending on the fire location, the amount of the overflow smoke exhibited either an inverted V-shaped variation or a monotonical increase with the door position. Multiple peaks in the smoke temperature below the tunnel ceiling is attributed to the uneven distribution of the overflow smoke. A dimensional analysis revealed a quantifiable relationship between the heat flow of the overflow smoke and the peak temperatures below the tunnel ceiling. Consequently, an empirical model was developed to predict the maximum smoke temperature below the tunnel ceiling under different heat release rates and longitudinal ventilation velocities. These findings are expected to enhance the understanding of carriage fires and provide a theoretical guidance for future ventilation and safety designs in subway systems.

Keywords: Carriage fire, Subway tunnel, Longitudinal ventilation, Lateral doors, Smoke overflow, Temperature distribution

1. Introduction

The subway system, rapidly developing and playing a crucial role in urban public transportation, has emerged as a solution to escalating congestion issues. Tunnels and carriages are integral components of the subway system, characterized by their narrow and confined structural features. In situations where a fire breaks out in a train carriage, a rapid increase in temperature and substantial smoke production occur, posing a significant threat to passenger safety. Statistically, toxic and

* Correspondence should be addressed to: Kun He, E-mail: hkky@ustc.edu.cn



high-temperature smoke accounts for approximately 85% of fatalities in building fires [1]. Therefore, studying the smoke propagation characteristics of a train carriage fire in a subway tunnel is of practical importance.

Over the recent years, numerous scholars have conducted extensive research into the tunnel fires, focusing primarily on the smoke movement characteristics and the control methods [2–10]. In contrast, the research on the train carriage fires commenced later, predominantly targeting the fire development under natural ventilation. Lonermark et al. [11] conducted a series of experiments using a 1:3 scale model of a train carriage to study the variations in the heat release rate (HRR), temperature field, and thermal radiation. They derived the evolution laws for control parameters during the initial stages of fire development. Shi et al. [12] further utilized a cone calorimeter system to evaluate the combustion behaviors in a full-scale carriage fire during the first three minutes of burning. Ng et al. [13] experimentally analyzed the flame color through the oxygen concentration method in a 1:15 scale model carriage with movable lateral openings under limited ventilation. Peng et al. [14–16] conducted reduced-scale tests to investigate flame patterns and smoke temperature in train carriage fires under various fire locations and opening conditions, and the similarities and differences between the carriage fires and the tunnel fires were compared.

In the scenarios where a train catches fire and stops in a tunnel using the longitudinal evacuation platform for safe evacuation, the lateral carriage doors complicates the smoke propagation in the tunnel due to the overflow behavior. Previous studies on this specific fire scenario have primarily focused on the smoke temperature characteristics in the tunnel space. Meng et al. [17] performed a series of model-scale experiments to analyze the smoke temperature distribution below the tunnel ceiling considering various platform-tunnel combination doors in the subway stations. Ren et al. [18] employed full-scale numerical simulations to study the smoke flow characteristics in the tunnel during a scenario with two simultaneous fires at the bottom of a carriage. Tang et al. [19] experimentally investigated the maximum smoke temperature below the tunnel ceiling in a carriage fire with a single lateral opening under the influence of ceiling smoke extraction. Zhang et al. [20] conducted model-scale experiments to assess the maximum smoke temperature below the tunnel ceiling during the blocking effect of a train carriage fire. Similarly, Shi et al. [21] analyzed the fire development process in a long- large tunnel with longitudinal ventilation through full-scale experiments, focusing mainly on the smoke temperature below the tunnel ceiling in various downstream zones, which was found to still adhere to the law of exponential decay.

However, the relationship between the overflow smoke at the lateral carriage doors and the smoke temperature distribution below the tunnel ceiling remains unclear. Cong et al. [22] introduced a hypothesis of an equivalent virtual fire source, conceptualizing the carriage fire as an intermediate scenario between tunnel and compartment fires. Utilizing the full-scale numerical simulations, the impact of smoke overflow behavior on smoke propagation in naturally ventilated tunnels was demonstrated. Yet, when the mechanical ventilation is operational, the overflow smoke aligns with the ventilation direction, resulting in significant fluctuations in the smoke propagation process. Therefore, this study further inves-

tigates the characteristics of smoke overflow at the lateral carriage doors and the smoke temperature beneath the tunnel ceiling in a longitudinally ventilated tunnel during a carriage fire. The research results are expected to be beneficial for the ventilation, evacuation, and rescue of the subway systems.

2. Research Methods

2.1. Scaling Law

When employing the scale modelling for studying, it is crucial to establish the similarity between different scales. Because the thermal plume in a building fire is predominantly driven by the buoyancy, the Froude scaling emerges as the most appropriate law in the fire research [23–25]. Table 1 presents several proportional relationships commonly used in the Froude scaling.

In this study, the 1:3 scaling ratio was selected for the experimental tests and numerical simulations. Referring the full-scale experiments conducted by Shi et al. [12] that the stable HRR is 1.84 MW, with a peak of 2.14 MW. Therefore, the HRR in the carriage ranges from 35.4 kW to 123.9 kW was selected, corresponding to 0.55–1.93 MW in full scale. In addition, four longitudinal ventilation velocity in the tunnel of 0.6–1.5 m/s was considered, corresponding to 1.04–2.6 m/s in full scale.

2.2. Experimental Tests

As depicted in Figure 1, a model-scale subway fire test bench, replicating the Hefei Metro in China, was constructed and comprised of a tunnel and train. The horseshoe-shaped tunnel, measuring 30 m in length and 1.6 m in width, features an arc ceiling 0.6 m high, made of stainless steel. The vertical sidewalls below the arc ceiling are constructed from 10 mm thick fireproof board and 8 mm thick fireproof glass. The simplified train is composed of two carriages and made of 10 mm thick fireproof board. The upper rectangular space measures 13.2 m in length, 0.9 m in width, and 0.7 m in height, sitting on the ground via a 0.4 m high brackets. To simulate actual lateral open doors, eight evenly spaced openings, each measuring 0.4 m in width and 0.6 m in height, were created on one side of the carriage.

The fire source, a square propane burner with 0.25 m sides, was positioned at the center of the carriage floor, maintaining an effective height of 0.65 m from the burner surface to the carriage ceiling. The HRR can be calculated by multiplying the mass flow rate with the heat of combustion (44.1 kJ/kg) of the fuel gas. A 3 m long rectified segment seamlessly connected the frequency converter fan to the model tunnel. Four anemometers, positioned upwind of the carriage, measured the longitudinal ventilation rate in the tunnel. Smoke temperature was monitored using two sets of horizontal K-type thermocouples placed 1.5 cm below the tunnel and carriage ceilings along the longitudinal centerline. To capture the data in the quasi-steady state of fire development, each test time was maintained for 1000 s

Table 1
Proportional Relation Commonly Used in Froude Scaling

Parameter	Proportional relation
Mass flow rate (kg/s)	$m_F/m_M = (L_F/L_M)^3$
Heat flow (kW)	$Q_F/Q_M = (L_F/L_M)^{5/2}$
Velocity (m/s)	$V_F/V_M = (L_F/L_M)^{1/2}$
Temperature (K)	$T_F/T_M = 1$
Time (s)	$t_F/t_M = (L_F/L_M)^{1/2}$

M model-scale F full-scale L length

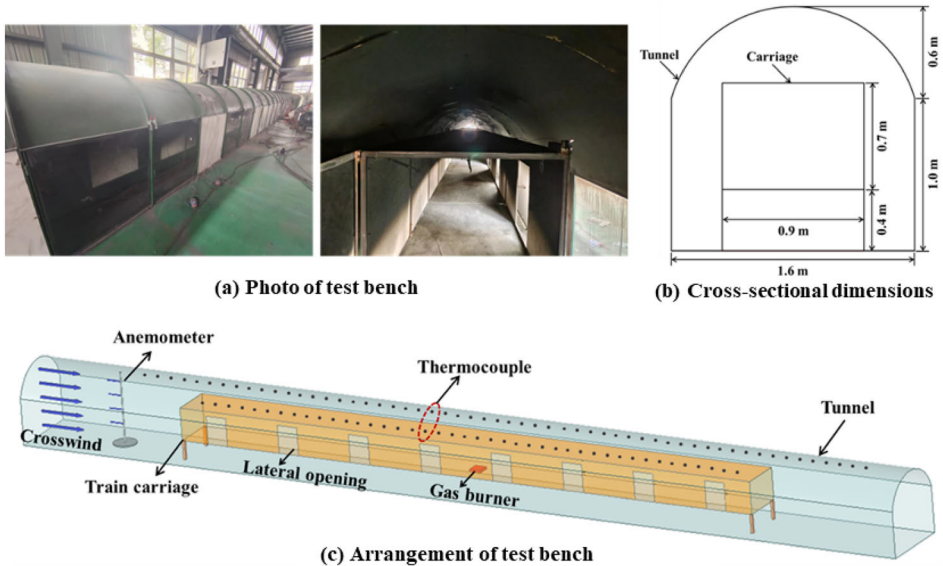


Figure 1. Schematic diagram of experimental bench.

and the average results during the final 30 s used for analysis. The detailed experimental conditions are provided in Table 2.

2.3. Numerical Simulation

Numerical simulation is an effective tool for obtaining the parameters difficult to measure in experiments. It can also reveal flow details not visible in experimental settings, thereby facilitating a clearer understanding of the fire development process. In this study, the Fire Dynamic Simulator (FDS, version 6.6.0), a widely-used software specifically designed for modeling smoke and heat transport from fires [26], was employed to analyze the smoke overflow characteristics at the lateral carriage doors.

As shown in Figure 2, the dimensions and materials of the FDS model are consistent with those of the model-scale experimental bench. The tunnel ends were

Table 2
Summary of Experimental Scenarios

Test No	HRR (kW)	Ventilation rate (m/s)	Fire location*
1–4	35.4	0.6, 0.9, 1.2, 1.5	$d = 0$ m
5–8	53.1	0.6, 0.9, 1.2, 1.5	$d = 0$ m
9–12	70.8	0.6, 0.9, 1.2, 1.5	$d = 0$ m
13–16	88.5	0.6, 0.9, 1.2, 1.5	$d = 0$ m
17–20	106.2	0.6, 0.9, 1.2, 1.5	$d = 0$ m

* d is the distance from the fire source to the middle of carriage

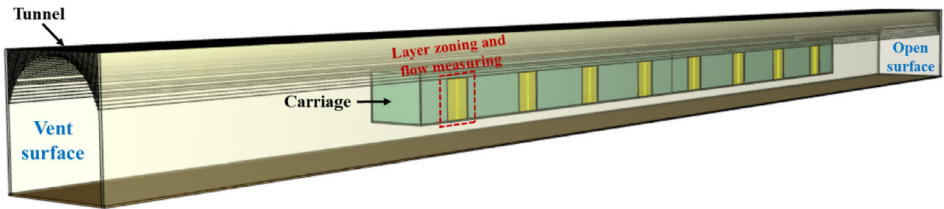


Figure 2. Schematic diagram of numerical model.

designated as “Supply” and “Open” surfaces, respectively. Devices for measuring flow and layer zoning were installed at each carriage door to record the mass flow rate, layer height, and average layer temperature. Due to the simplification of carriage model in this study, additional consideration was given to the influence of the fire source location on the smoke overflow behavior in order to obtain universal conclusions. Moreover, in accordance with the principle of minimizing the number of evacuation personnel along the ventilation direction [27], six fire locations spaced 0 to 5 m along the longitudinal centerline of the downstream half of the carriage with an HRR of 123.9 kW and a longitudinal ventilation rate of 1.2 m/s were considered.

Grid size is a crucial factor for the accuracy of numerical simulation. Huang et al. [28] found that when the mesh size equals to 0.1 times the characteristic diameter of the fire source, i.e. $\delta x = 0.1D^*$, a good agreement between simulation and experiment can be achieved. The characteristic diameter of the fire source is defined as:

$$D^* = \left(\frac{Q}{\rho_0 c_p T_0 \sqrt{g}} \right)^{2/5} \quad (1)$$

where Q is the HRR of the fire source, kW; ρ_0 is the ambient density, kg/m^3 ; c_p is the specific heat of air at constant pressure, $\text{kJ}/(\text{kg}\cdot\text{K})$; T_0 is the ambient temperature, K; and g is the gravity acceleration, m/s^2 .

The characteristic diameter of the fire source can be determined ranging 0.253–0.417 m according to Table 2. Consequently, a mesh size of 0.03 m was selected

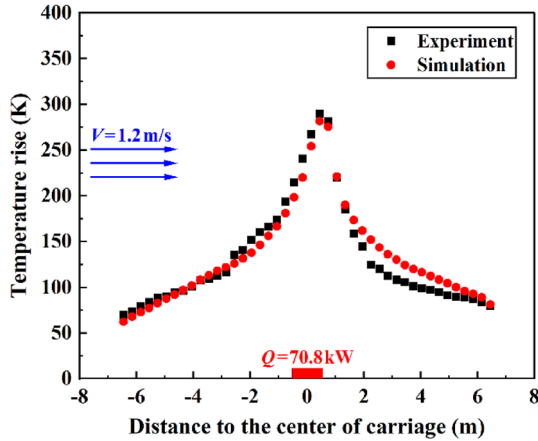


Figure 3. Comparison of the smoke temperature below the carriage ceiling between simulations and experiments.

for the numerical simulations. To validate the accuracy of the numerical model, a comparison of the smoke temperatures below the carriage ceiling from both simulations and experiments was conducted, particularly when the fire source is located at the center of the carriage. As depicted in Figure 3, a negative abscissa signifies the upwind direction, and the opposite for a positive sign. The similarity in comparison results further substantiates the reliability and accuracy of the simulation outcomes.

3. Results and Discussion

3.1. Smoke Overflow Characteristics at the Lateral Carriage Doors

When a fire occurs in the carriage, the lateral doors serve as the only safe exit for passengers to evacuate. Therefore, analyzing the overflow characteristics of the smoke at the lateral doors is of significant importance for assessing the fire hazards. For the convenience of representation, the scenario same with experiments is labeled as “Scenario A”, and the scenario involving the variations in the fire location is labeled as “Scenario B”. Figure 4 depicts the mass flow rates of the overflow gas at the lateral carriage doors, which can be categorized into two zones based on the door position. In the zone upwind of the fire source, the mass flow rates at different doors are relatively constant and slightly above zero, suggesting this zone functions as an intake area for wind flow. Conversely, in the zone downstream of the fire source, the mass flow rate of the overflow gas consistently rises in the direction of the wind. In addition, both the increased HRR or longitudinal ventilation rate contribute to a rise in the mass flow rate, indicating that the downstream doors serve not only as an exhaust zone for the hot smoke but also the cold air.

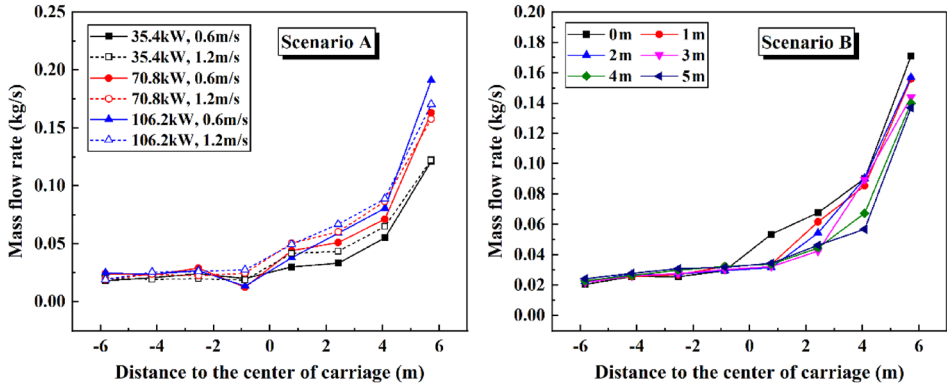


Figure 4. Mass flow rates of the overflow gas.

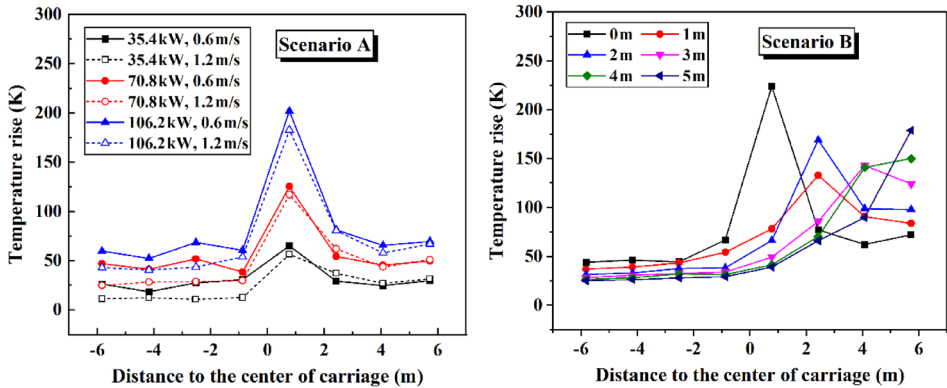


Figure 5. Average layer temperature rises of the overflow smoke.

Figure 5 presents the average temperature rises of the overflow smoke at the lateral carriage doors. The temperature of the overflow smoke displays an inverted V-shaped pattern with the door position, with the peak occurring at the first door downstream of the fire source. The longitudinal ventilation significantly reduces the temperature of the overflow smoke upstream of the fire source. However, the influence of longitudinal ventilation and HRR on the temperature of the overflow smoke is minor in the zone downstream of the fire source.

Figure 6 presents the layer heights of the overflow smoke at the lateral carriage doors. It can be observed that the smoke layer height initially increases and then decreases along the ventilation direction, and the apex position depends on the ventilation velocity and basically appears at the adjacent door of the fire source. Additionally, the smoke layer height is basically independent of the HRR except for the condition where the HRR is 35.4 kW and the longitudinal ventilation velocity is 1.2 m/s because of the poor smoke stratification. For a fixed HRR, an

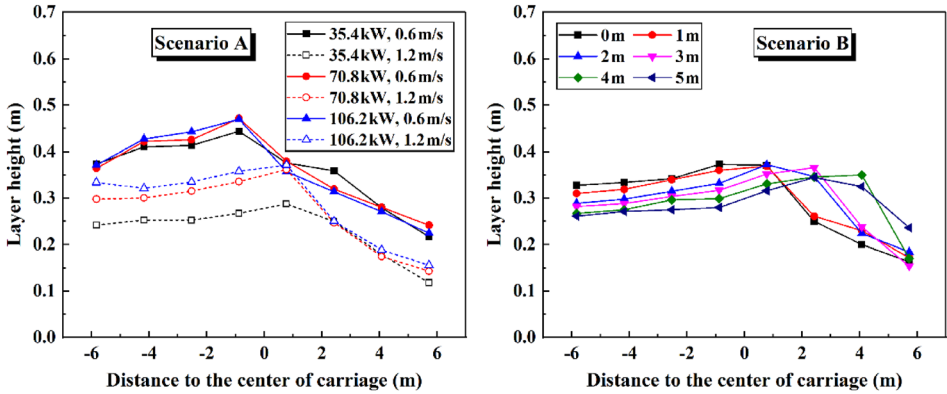


Figure 6. Layer heights of the overflow smoke at the lateral carriage doors.

increase in longitudinal ventilation velocity intensifies the disturbance to the smoke stratification, resulting in a reduction in the smoke layer height.

Considering the aforementioned parameters, heat flow was proposed as a comprehensive metric to quantify the amount of overflow smoke. The carriage fire investigated in this paper is characterized as a fuel-controlled (well-ventilated) fire. Consequently, the heat flow of the overflow smoke at the lateral door can be calculated using the following formula:

$$q_s = c_p m_s \Delta T_s \quad (2)$$

where m_s is the mass flow rate of the overflow smoke, kg/s; and ΔT_s is the temperature rise of the overflow smoke, K.

Due to the overflow gas comprising both cold air and hot smoke, directly calculating the heat flow of the overflow smoke using the data from Figure 4 may yield an exaggerated result. To address this, the study adopted the hypothesis that the local area around each carriage door can be approximated as a compartment with a single opening [29]. This allows for the calculation of the mass flow rate of overflow smoke by referring to the dynamics of a compartment fire:

$$m_s = \frac{2}{3} C_d W_d \rho_a \sqrt{2g \frac{T_a}{T_s} \left(1 - \frac{T_a}{T_s}\right)} (H_d - H_s)^{3/2} \quad (3)$$

where C_d is the flow coefficient, which can be regarded as 0.6 [30]; W_d is the width of the lateral door, m; H_d is the height of the lateral door, m; and H_s is the smoke layer height at the lateral door, m.

Drawing on the simulation results regarding the height and average temperature of the smoke layer, Figure 7 compares the mass flow rates and heat flows of overflow smoke between calculated and simulated values. The calculations align closely with the numerical simulations, except for the end door downstream of the

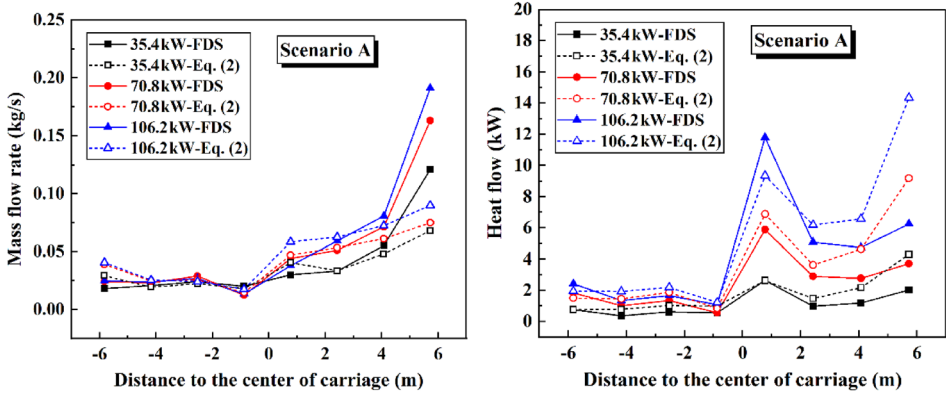


Figure 7. Comparison of mass flow rates and heat flows of the overflow smoke between calculations and simulations when $d = 0\text{ m}$ and $V = 0.6\text{ m/s}$.

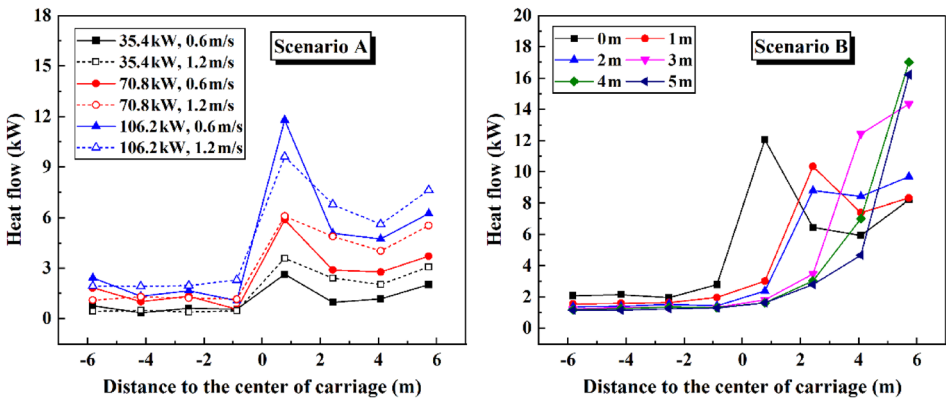


Figure 8. Heat flows of the overflow smoke at the lateral carriage doors.

fire source. At this location, the ejection of a large amount of cold air along with hot smoke from the carriage leads to a notable discrepancy in both the mass flow rate and heat flow.

Figure 8 displays the calculated heat flows of overflow smoke at the lateral carriage doors. Overall, the smoke in the carriage overflows from the downstream doors under the influence of the longitudinal ventilation, in which the amount of the overflow smoke initially decreases and then increases at the final two doors along the ventilation direction. Obviously, when the fire source is located downstream of the third to last lateral door, the amount of overflow smoke monotonically increases along the ventilation direction. With the increase in ventilation velocity, more smoke is carried downstream, resulting in a decrease in overflow smoke at the first downstream door and an increase at the doors further down-

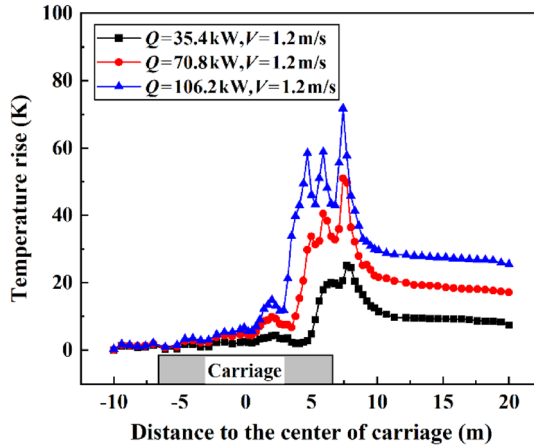


Figure 9. Longitudinal distribution of the smoke temperature below the tunnel ceiling.

stream. However, regarding the condition where the HRR is 35.4 kW and the longitudinal ventilation velocity is 1.2 m/s, an increase in overflow smoke was noted at the first downstream door. This increment is attributed to the upstream smoke with poor stratification overflows from this door with the airflow.

3.2. Smoke Temperature Below the Tunnel Ceiling

The smoke temperatures measured in the experimental tests when the fire source is located at the center of the carriage are analyzed in this section. Once the smoke overflows from the carriage doors, it accumulates and spreads below the tunnel ceiling. Figure 9 shows the typical longitudinal distribution of smoke temperature below the tunnel ceiling. It is evident that due to the uneven distribution of overflow smoke, which primarily exits into the tunnel from the doors downstream of the fire source, the smoke backflow in the tunnel is nearly eliminated. Additionally, the phenomenon of multiple peak values in the smoke temperature can be observed downstream of the fire source.

Table 3 summarizes the peak smoke temperatures and their locations below the tunnel ceiling when the fire source is located at the center of the carriage. These data are segmented into four parts based on the door location downstream of the fire source. Since the number of peak temperatures is at most equivalent to the number of downstream doors, a one-to-one correspondence between them can be inferred. With a given HRR, an increase in the longitudinal ventilation rate tends to gradually eliminate the characteristic of the multiple peak temperatures along the ventilation direction. As inferred from Figure 8b, a monopolar temperature characteristic is likely to emerge when the fire source is located downstream of the third to last lateral door.

Figure 10 shows the peak smoke temperature rises below the tunnel ceiling under different heat flows of the overflow smoke at the lateral carriage doors. It is

Table 3
Summary of the Peak Smoke Temperature Rise and Its Position Below the Tunnel Ceiling

V (m/s)	$\Delta T_p, \Delta x_0$ (K, m)				
	35.4 kW	53.1 kW	70.8 kW	88.5 kW	106.2 kW
0.6	27.7, 2.6	41.9, 2.6	56.3, 2.3	97.8, 2	121.6, 2
	31.2, 4.7	38.6, 4.7	53.1, 4.7	65.6, 4.7	73, 4.7
	38.9, 5.9	45.2, 5.9	59.8, 5.9	74.5, 5.6	80.1, 5.6
	33.1, 7.1	43.4, 7.1	55.6, 7.1	66.8, 7.1	72.6, 6.8
0.9	—	—	48.1, 2.9	60.1, 2.9	82.5, 2.6
	26.8, 4.7	40.7, 4.4	46.8, 4.4	49.1, 4.4	55.7, 4.4
	25.1, 5.9	31.8, 5.9	43, 6.2	54.7, 6.2	67.9, 6.2
	30.9, 7.4	43.6, 7.4	54.1, 7.1	60.8, 6.8	70.8, 6.8
1.2	—	—	—	—	—
	—	—	33.8, 5	45.7, 4.7	58.6, 4.7
	20.1, 6.5	29.8, 5.9	40.5, 5.9	50.9, 5.9	58.9, 5.9
	25.2, 7.7	39.5, 7.7	51.1, 7.4	61.5, 7.4	71.9, 7.4
1.5	—	—	—	—	—
	—	—	—	—	—
	—	—	—	—	47.3, 6.8
	20.5, 8.9	27.8, 8.6	36.3, 8	47.9, 8	59, 8

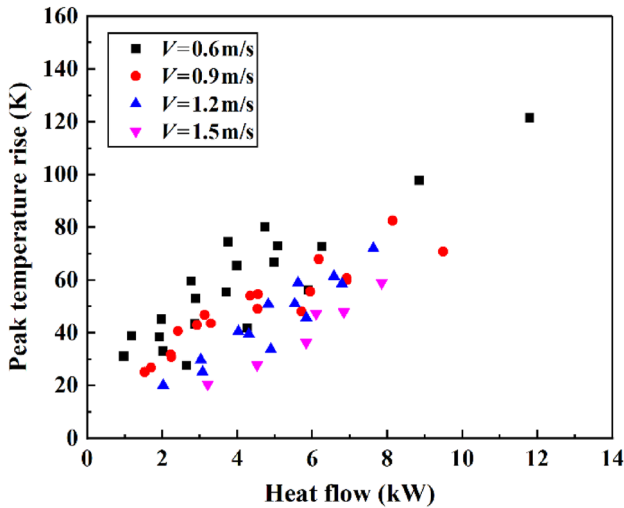


Figure 10. Peak smoke temperature rises below the tunnel ceiling under different heat flows of the overflow smoke.

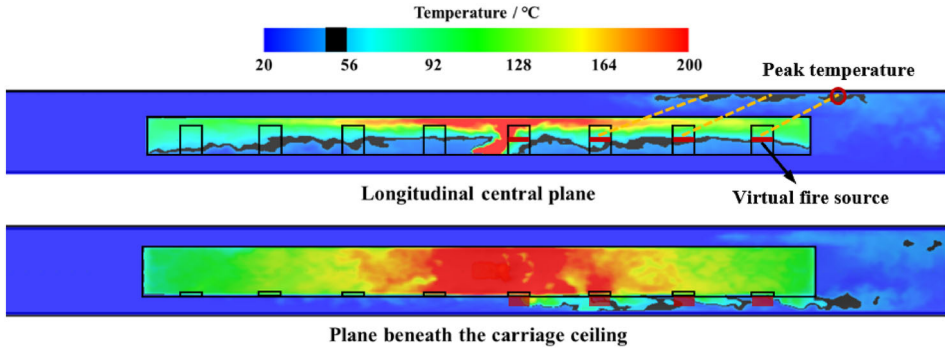


Figure 11. Temperature fields when $Q = 70.8 \text{ kW}$ and $V = 1.2 \text{ m/s}$.

evident that these data points converge and ascend with the increase in heat flow for a specific longitudinal ventilation rate. This relationship can be expressed by the following function:

$$\Delta T_p = f(q, V, c_p, \rho_0, T_0, g, H_{ef}) \tag{4}$$

where H_{ef} is the effective height from the burner surface of the fire source to the tunnel ceiling, m; and q is the heat flow of the overflow smoke, kW.

In a model-scale tunnel with longitudinal ventilation, Kurioka et al. [31] established an empirical model to predict the maximum smoke temperature below the tunnel ceiling, which is expressed as follows:

$$\frac{\Delta T_{\max}}{T_0} = \gamma \left(\frac{Q^{*2/3}}{Fr^{1/3}} \right)^\varepsilon \tag{5}$$

$$\begin{aligned} Q^{*2/3}/Fr^{1/3} < 1.35, \gamma = 1.77, \varepsilon = 6/5 \\ Q^{*2/3}/Fr^{1/3} \geq 1.35, \gamma = 2.54, \varepsilon = 0 \end{aligned} \tag{6}$$

where Q^* is the dimensionless heat release rate of the fire source, which is defined as $Q^* = Q / (\rho_0 c_p T_0 g^{1/2} H_{ef}^{5/2})$; and Fr is the Froude number, defined as $Fr = V^2 / (gH_{ef})$.

As shown in Figure 11, assuming that the overflow smoke at each door as a virtual fire source and the peak smoke temperature below the tunnel ceiling is contributed by the heat flow of the overflow smoke at its corresponding door, Equation (4) can be rearranged referring to Equation (5) as:

$$\frac{\Delta T_p}{T_0} = \alpha \left(\frac{q^{*2/3}}{Fr^{1/3}} \right)^\beta \tag{7}$$

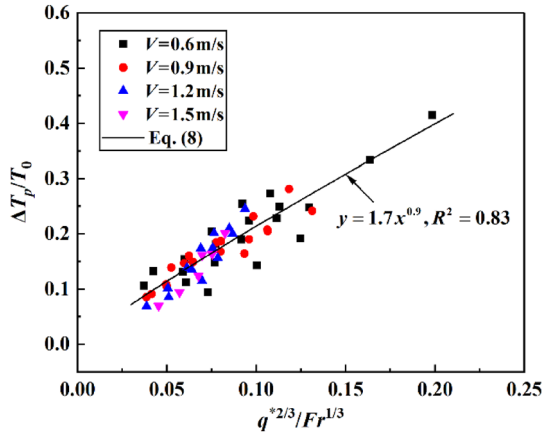


Figure 12. Relationship between the dimensionless peak smoke temperature below the tunnel ceiling and the variable of $q^{*2/3}/Fr^{1/3}$.

where α and β are the coefficients; q^* is the dimensionless heat flow of the overflow smoke, defined as $q^* = q / (\rho_0 c_p T_0 g^{1/2} h_{ef}^{5/2})$; h_{ef} is the effective height from the neutral plane at the lateral door, usually 0.5 times the opening height for a compartment fire with single lateral opening [32], to the tunnel ceiling, m.

The relationship between the dimensionless peak smoke temperature rise below the tunnel ceiling and the variable of $q^{*2/3}/Fr^{1/3}$ is shown in Figure 12. It is obviously that all data points have a good convergence after dimensionless processing, which can be well correlated with $\alpha = 1.7$ and $\beta = 0.9$. Consequently, Equation (7) can be rewritten as:

$$\frac{\Delta T_p}{T_0} = 1.7 \left(\frac{q^{*2/3}}{Fr^{1/3}} \right)^{0.9} \tag{8}$$

From an engineering perspective, it is more important to quickly predict the maximum smoke temperature below the tunnel ceiling based on the existing boundary conditions. Figure 13 presents the relationship between the dimensionless maximum smoke temperature rise below the tunnel ceiling and the variable of $(Q^{*2/3}/Fr^{1/3})^{6/5}$ based on Equation (5). It is obviously that all data points agree well with a linear function with a slope of 0.825, can be given by:

$$\frac{\Delta T_{max}}{T_0} = 0.825 \left(\frac{Q^{*2/3}}{Fr^{1/3}} \right)^{6/5} \tag{9}$$

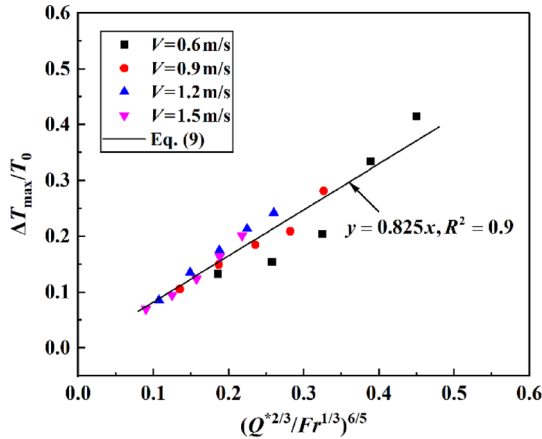


Figure 13. Relationship between the dimensionless maximum smoke temperature below the tunnel ceiling and the variable of $(Q^{2/3}/Fr^{1/3})^{6/5}$.

4. Conclusions

In this study, both experimental and numerical methods were used to investigate the smoke overflow characteristics at the lateral carriage doors and the smoke temperature below the tunnel ceiling in a longitudinally ventilated tunnel during a carriage fire. The main findings are summarized as follows:

- (1) Relative to the parameters such as mass flow rate, smoke layer height, and average smoke layer temperature, the heat flow proves to be a more appropriate measure for quantifying the amount of overflow smoke. Predominantly, smoke within the carriage overflows from the lateral doors downstream of the fire source, especially the first and last two downstream doors.
- (2) The uneven distribution of the overflow smoke at the lateral carriage doors leads to the multiple peaks in the smoke temperature below the tunnel ceiling. The number of these peak temperatures is at most equal to the number of downstream carriage doors. With a given HRR, an increase in the longitudinal ventilation rate tends to gradually eliminate the multiple peak temperatures along the ventilation direction, until evolves into a monopolar temperature.
- (3) By treating the overflow smoke at each door as a virtual fire source, an empirical model was developed to correlate these peak temperatures with the heat flow of the overflow smoke, based on dimensional analysis. Additionally, a dimensionless model was proposed for predicting the maximum smoke temperature below the tunnel ceiling when the fire source is located at the center of the carriage.

Acknowledgements

This work was funded by Natural Science Research Project of Anhui Educational Committee (2022AH050823), Scientific Research Foundation for High-level Talents of Anhui University of Science and Technology (2022yjrc110), and National Key R&D Program of China under Grant (No. 2022YFC3005201). We sincerely appreciate these supports.

Author Contributions

WC: Conceptualization, Writing—Original Draft, Funding Acquisition. XC: Investigation. LS: Writing—Review & Editing. KH: Supervision, Funding Acquisition.

References

1. Ji J, Tan T, Gao Z, Wan H, Zhu J, Ding L (2019) Numerical investigation on the influence of length–width ratio of fire source on the smoke movement and temperature distribution in tunnel fires. *Fire Technol* 55:963–979. [10.1007/s10694-018-00814-4](https://doi.org/10.1007/s10694-018-00814-4)
2. Weng M, Lu X, Liu F, Du C (2016) Study on the critical velocity in a sloping tunnel fire under longitudinal ventilation. *Appl Therm Eng* 94:422–434. [10.1016/j.applthermaling.2015.10.059](https://doi.org/10.1016/j.applthermaling.2015.10.059)
3. Tang F, He Q, Mei F, Wang Q, Zhang H (2018) Effect of ceiling centralized mechanical smoke exhaust on the critical velocity that inhibits the reverse flow of thermal plume in a longitudinal ventilated tunnel. *Tunn Undergr Space Technol* 82:191–198. [10.1016/j.tust.2018.08.039](https://doi.org/10.1016/j.tust.2018.08.039)
4. Ji J, Wang Z, Ding L, Yu L, Gao Z, Wan H (2019) Effects of ambient pressure on smoke movement and temperature distribution in inclined tunnel fires. *Int J Therm Sci* 145:106006. [10.1016/j.ijthermalsci.2019.106006](https://doi.org/10.1016/j.ijthermalsci.2019.106006)
5. Huang Y, Li Y, Li J, Dong B, Bi Q, Li Y, Li J (2019) Experimental investigation on temperature profile with downstream vehicle in a longitudinally ventilated tunnel. *Exp Therm Fluid Sci* 103:149–156. [10.1016/j.expthermflusci.2019.01.006](https://doi.org/10.1016/j.expthermflusci.2019.01.006)
6. Chen C, Zhang Y, Lei P, Jiao W (2020) A study for predicting the maximum gas temperature beneath ceiling in sealing tactics against tunnel fire. *Tunn Undergr Space Technol* 98:103275. [10.1016/j.tust.2019.103275](https://doi.org/10.1016/j.tust.2019.103275)
7. Guo Q, Zhu H, Zhang Y, Yan Z (2020) Theoretical and experimental studies on the fire-induced smoke flow in naturally ventilated tunnels with large cross-sectional vertical shafts. *Tunn Undergr Space Technol* 99:103359. [10.1016/j.tust.2020.103359](https://doi.org/10.1016/j.tust.2020.103359)
8. He K, Shi L, Zhang S, Cong W, Yang H, Cheng X (2023) Experimental study on temperature attenuation of smoke flow driven by dual fire sources in a tunnel. *Tunn Undergr Space Technol* 134:105004. [10.1016/j.tust.2023.105004](https://doi.org/10.1016/j.tust.2023.105004)
9. Li Q, Kang J, Wu Y, Luo J (2022) Theoretical and numerical study of smoke back-layering length for an inclined tunnel under longitudinal ventilation. *Fire Technol* 58:2143–2166. [10.1007/s10694-022-01250-1](https://doi.org/10.1007/s10694-022-01250-1)
10. Li Z, Zhang Y, Jiang H, Tang C, Luo D, Chen L, Lin Y, Li T (2022) Effect of fire source elevation on the smoke spreading characteristics in an extra-long tunnel. *Fire Technol* . [10.1007/s10694-022-01299-y](https://doi.org/10.1007/s10694-022-01299-y)

11. Lönnermark A, Ingason H, Li YZ, Kumm M (2017) Fire development in a 1/3 train carriage mock-up. *Fire Saf J* 91:432–440. [10.1016/j.firesaf.2017.03.016](https://doi.org/10.1016/j.firesaf.2017.03.016)
12. Shi C, Zhong M, Chen C, Jiao W, Li J, Zhang Y, Zhang L, Li Y, He L (2020) Metro train carriage combustion behaviors – Full-scale experiment study. *Tunn Undergr Space Technol* 104:103544. [10.1016/j.tust.2020.103544](https://doi.org/10.1016/j.tust.2020.103544)
13. Ng YW, Chow WK, Cheng CH, Chow CL (2019) Scale modeling study on flame colour in a ventilation-limited train car pool fire. *Tunn Undergr Space Technol* 85:375–391. [10.1016/j.tust.2018.12.026](https://doi.org/10.1016/j.tust.2018.12.026)
14. Peng M, Cheng X, Cong W, Yang H, Shahid MU, Yuen R, Zhang H (2021) Experimental study on temperature profile in long-narrow compartment fire with multiple lateral openings. *Tunn Undergr Space Technol* 117:104018. [10.1016/j.tust.2021.104018](https://doi.org/10.1016/j.tust.2021.104018)
15. Peng M, Cheng X, Cong W, Yuen R (2020) Experimental investigation on temperature profiles at ceiling and door of subway carriage fire. *Fire Technol* 57:439–459. [10.1007/s10694-020-01010-z](https://doi.org/10.1007/s10694-020-01010-z)
16. Peng M, Shi L, He K, Yang H, Cong W, Cheng X, Richard Y (2020) Experimental study on fire plume characteristics in a subway carriage with doors. *Fire Technol* 56:401–423. [10.1007/s10694-019-00882-0](https://doi.org/10.1007/s10694-019-00882-0)
17. Meng N, Wang Q, Liu Z, Li X, Yang H (2017) Smoke flow temperature beneath tunnel ceiling for train fire at subway station: Reduced-scale experiments and correlations. *Appl Therm Eng* 115:995–1003. [10.1016/j.applthermaleng.2017.01.027](https://doi.org/10.1016/j.applthermaleng.2017.01.027)
18. Ren F, Shi C, Li J, Che H, Xu X (2021) Numerical study on the flow characteristics and smoke temperature evolution under double fires condition with a metro train in tunnel. *Tunn Undergr Space Technol* 114:103943. [10.1016/j.tust.2021.103943](https://doi.org/10.1016/j.tust.2021.103943)
19. Tang F, He Q, Chen L, Li P (2019) Experimental study on maximum smoke temperature beneath the ceiling induced by carriage fire in a tunnel with ceiling smoke extraction. *Sustain Cities Soc* 44:40–45. [10.1016/j.scs.2018.09.026](https://doi.org/10.1016/j.scs.2018.09.026)
20. Zhang H, Sun J, Zhang G, Zhou X, Pan Y (2021) Experimental study on the tunnel temperature distribution under the coupling effect of train blocking and fire inside the carriage. *Tunn Undergr Space Technol* 112:103915. [10.1016/j.tust.2021.103915](https://doi.org/10.1016/j.tust.2021.103915)
21. Shi C, Li J, Xu X (2021) Full-scale tests on smoke temperature distribution in long-large subway tunnels with longitudinal mechanical ventilation. *Tunn Undergr Space Technol* . [10.1016/j.tust.2020.103784](https://doi.org/10.1016/j.tust.2020.103784)
22. Cong W, Shi L, Shi Z, Peng M, Yang H, Zhang S, Cheng X (2020) Effect of train fire location on maximum smoke temperature beneath the subway tunnel ceiling. *Tunn Undergr Space Technol* 97:103282. [10.1016/j.tust.2020.103282](https://doi.org/10.1016/j.tust.2020.103282)
23. Fan C, Ji J, Li Y, Ingason H, Sun J (2017) Experimental study of sidewall effect on flame characteristics of heptane pool fires with different aspect ratios and orientations in a channel. *Proc Combust Inst* 36:3121–3129. [10.1016/j.proci.2016.06.196](https://doi.org/10.1016/j.proci.2016.06.196)
24. Guo F, Ding L, Gao Z, Yu L, Ji J (2020) Effects of wind flow and sidewall restriction on the geometric characteristics of propane diffusion flames in tunnels. *Energy* 198:117332. [10.1016/j.energy.2020.117332](https://doi.org/10.1016/j.energy.2020.117332)
25. Yao Y, He K, Peng M, Shi L, Cheng X (2021) The maximum gas temperature rises beneath the ceiling in a longitudinal ventilated tunnel fire. *Tunn Undergr Space Technol* 108:103672. [10.1016/j.tust.2020.103672](https://doi.org/10.1016/j.tust.2020.103672)
26. McGrattan K, Hostikka S, Floyd J, Vanella M, Craig W, Overholt K (2017) Fire dynamics simulator user’s guide sixth edition. NIST special publication 1019:1–339. <https://doi.org/10.6028/NIST.SP.1019>
27. Wang F, Liu F, Obadi I, Weng M (2021) Study on the smoke propagation characteristics of metro tunnel fire under the effects of piston wind. *Indoor Built Environ* 32:149–169. [10.1177/1420326X21998420](https://doi.org/10.1177/1420326X21998420)

28. Huang Y, Li Y, Dong B, Li J, Liang Q (2018) Numerical investigation on the maximum ceiling temperature and longitudinal decay in a sealing tunnel fire. *Tunn Undergr Space Technol* 72:120–130. [10.1016/j.tust.2017.11.021](https://doi.org/10.1016/j.tust.2017.11.021)
29. Delichatsios MA, Lee Y-P, Tofilo P (2009) A new correlation for gas temperature inside a burning enclosure. *Fire Saf J* 44:1003–1009. [10.1016/j.firesaf.2009.06.009](https://doi.org/10.1016/j.firesaf.2009.06.009)
30. Li M, Gao Z, Ji J, Li K, Sun J (2017) Wind effects on flame projection probability from a compartment with opposing openings. *Fire Saf J* 91:414–421. [10.1016/j.firesaf.2017.04.037](https://doi.org/10.1016/j.firesaf.2017.04.037)
31. Kurioka H, Oka Y, Satoh H, Sugawa O (2003) Fire properties in near field of square fire source with longitudinal ventilation in tunnels. *Fire Saf J* 38:319–340. [10.1016/S0379-7112\(02\)00089-9](https://doi.org/10.1016/S0379-7112(02)00089-9)
32. Lee YP, Delichatsios MA, Silcock GWH (2007) Heat fluxes and flame heights in façades from fires in enclosures of varying geometry. *Proc Combust Inst* 31:2521–2528. [10.1016/j.proci.2006.08.033](https://doi.org/10.1016/j.proci.2006.08.033)

Publisher's Note Springer Nature remains neutral with regard to jurisdictional claims in published maps and institutional affiliations.

Springer Nature or its licensor (e.g. a society or other partner) holds exclusive rights to this article under a publishing agreement with the author(s) or other rightsholder(s); author self-archiving of the accepted manuscript version of this article is solely governed by the terms of such publishing agreement and applicable law.